AIP | Journal of Applied Physics

Mn doping-induced structural and magnetic transformations in the antiferroelectric phase of the Bi1−xNdxFeO3 perovskites

V. A. Khomchenko, I. O. Troyanchuk, T. M. R. Maria, D. V. Karpinsky, S. Das et al.

Citation: J. Appl. Phys. **112**, 064105 (2012); doi: 10.1063/1.4752277
View online: http://dx.doi.org/10.1063/1.4752277
View Table of Contents: http://jap.aip.org/resource/1/JAPIAU/v112/i6
Published by the American Institute of Physics.

Mn doping-induced structural and magnetic transformations in the antiferroelectric phase of the $Bi_{1-x}Nd_xFeO_3$ perovskites

V. A. Khomchenko,[1,a)] I. O. Troyanchuk,[2] T. M. R. Maria,[3] D. V. Karpinsky,[4] S. Das,[5] V. S. Amaral,[5] and J. A. Paixão[1]
[1]*CEMDRX/Department of Physics, University of Coimbra, P-3004-516 Coimbra, Portugal*
[2]*SSPA "Scientific-Practical Materials Research Centre of NAS of Belarus," P. Brovka Street 19, 220072 Minsk, Belarus*
[3]*CQC/Department of Chemistry, University of Coimbra, P-3004-535 Coimbra, Portugal*
[4]*CICECO/Department of Materials and Ceramic Engineering, University of Aveiro, P-3810-193 Aveiro, Portugal*
[5]*CICECO/Department of Physics, University of Aveiro, P-3810-193 Aveiro, Portugal*

(Received 5 July 2012; accepted 9 August 2012; published online 17 September 2012)

X-ray diffraction, differential scanning calorimetry, and magnetization measurements of the $Bi_{0.825}Nd_{0.175}Fe_{1-y}Mn_yO_3$ ($y \leq 0.3$) compounds were carried out to follow the effect of Mn doping on the crystal structure and magnetic properties of the intermediate antiferroelectric and weak ferromagnetic phase of the $Bi_{1-x}Nd_xFeO_3$ perovskites. Suppression of the antipolar displacements typical of the parent *B*-site undoped compound followed by stabilization of the $GdFeO_3$-type structure as well as decrease of the antipolar-to-nonpolar transition temperature were found in this series with increasing Mn content. Compositional variation of the spontaneous magnetization in the $Bi_{0.825}Nd_{0.175}Fe_{1-y}Mn_yO_3$ ($y \leq 0.3$) system was shown to have a temperature-dependent character. At room temperature, a close to linear decrease of the spontaneous magnetization takes place with increase of the Mn content. At low temperatures, enhancement of the magnetization is observed with increasing the dopant concentration. © *2012 American Institute of Physics*. [http://dx.doi.org/10.1063/1.4752277]

I. INTRODUCTION

Multiferroics, in which magnetic order and ferroelectric polarization can be combined in a single phase, have been an object of growing interest.[1] Indeed, multiferroic materials with significant magnetoelectric coupling might open promising opportunities for designing novel microelectronic and spintronics devices. However, most magnetic ferroelectrics possess magnetic ordering at low temperature and are often antiferromagnets, in which the magnetoelectric effect is intrinsically small. $BiFeO_3$ perovskite,[2] in which the stereochemical activity of the $Bi^{3+}(6s^2)$ lone electron pairs induces appearance of the ferroelectric polarization, while the superexchange interactions Fe^{3+}-O-Fe^{3+} give rise to the G-type antiferromagnetic order, seems to be the most suitable object for multiferroic research in view of its high magnetic and ferroelectric transition temperatures ($T_N \sim 640$ K, $T_C \sim 1100$ K). On the other hand, spiral spin modulation, superimposed on the antiferromagnetic spin ordering,[3] cancels out any magnetization on a macroscopic scale and inhibits the observation of linear magnetoelectric effect.[4] Possibility to modify the multiferroic behavior of bismuth ferrite via *A*-site chemical substitution[5] motivated numerous investigations of crystal structure and physical properties of the $BiFeO_3$-based solid solutions. Recent investigations of the $Bi_{1-x}Nd_xFeO_3$ system have shown that the substitution-induced transition from the polar rhombohedral antiferromagnetic phase characteristic of $BiFeO_3$ (S.G. *R3c*) to the nonpolar orthorhombic weak ferromagnetic phase typical of $NdFeO_3$ (S.G. *Pnma*) occurs via the formation of the intermediate orthorhombic weak ferromagnetic phase (stable at $0.15 \leq x \leq 0.2$) combining the $NaNbO_3$-like[6] octahedral tilting and $PbZrO_3$-like[7] antipolar displacements of the *A*-site cations (S.G. *Pnam*).[8,9] Unlike lanthanide-doped series, $BiFe_{1-y}Mn_yO_3$ solid solutions cannot be prepared at ambient pressure in the entire composition range and exist in a single-phase state only at $y \leq 0.3$.[10] Mn substitution does not change structural symmetry of $BiFeO_3$, but significantly decreases the temperatures of the ferroelectric and magnetic phase transitions (near 6 °C per 1% Mn).[10] The manganese containing perovskites easily accommodate superstoichiometric oxygen, charge balance being achieved by the partial oxidation of Mn^{3+} to Mn^{4+}.[10] It has been recently found that simultaneous *Ln* (*Ln* = La, Pr, or Sm) and Mn substitution effectively modifies the initial polar rhombohedral (*R3c*) and intermediate antipolar orthorhombic (*Pnam*) structures to stabilize the phases either demonstrating incommensurate modulation or possessing nonpolar *Imma* or *Pnma* structures.[11–14] In this paper, we continue the investigation of $Bi_{1-x}Ln_xFe_{1-y}Mn_yO_3$ series and report on the effect of the Mn doping on the crystal structure and magnetic properties of the antiferroelectric and weak ferromagnetic $Bi_{0.825}Nd_{0.175}FeO_3$.[9]

II. EXPERIMENTAL

Ceramic samples $Bi_{0.825}Nd_{0.175}Fe_{1-y}Mn_yO_3$ ($0.1 \leq y \leq 0.3$) were prepared by a conventional solid-state reaction method using the high-purity oxides Bi_2O_3, Nd_2O_3 (annealed at 1000 °C), Fe_2O_3, and Mn_2O_3 taken in stoichiometric

a)Author to whom correspondence should be addressed. E-mail: uladzimir@fis.uc.pt. Telephone: +351 239 410 637. Fax: +351 239 829 158.

cation ratio and thoroughly mixed using a planetary mill (Retsch). The synthesis was carried out in air in a temperature range 900–950 °C for 15 h (annealing temperature was decreased with increasing Mn content). Room-temperature x-ray diffraction (XRD) patterns were collected using DRON-3M and Rigaku D/MAX-B diffractometers with Cu K_α radiation. High-temperature XRD measurements were carried out with a Philips X'Pert MPD diffractometer (Cu K_α radiation). The data were analysed by the Rietveld method using the FULLPROF program.[15] Differential scanning calorimetry was performed with a Pyris1 DSC (Perkin-Elmer) from 25 °C to 350 °C with a heating/cooling rate of 20 °C/min. Magnetization measurements at room and cryogenic (T = 5 K) temperatures were carried out with a vibrating sample magnetometer (Cryogenic Instruments) in the magnetic fields up to 10 T.

III. RESULTS AND DISCUSSION

In the intermediate antiferroelectric phase typical of the $Bi_{1-x}Ln_xFeO_3$ perovskites, the modulated $(a^-a^-c^+)$/$(a^-a^-c^-)$ octahedral tilting (in Glazer's notation[16]) superimposed on the $PbZrO_3$-like antipolar cationic displacements gives rise to the $\sqrt{2}a_c \times 2\sqrt{2}a_c \times 4a_c$ superstructure ($a_c \sim 4$ Å is the parameter of the cubic perovskite subcell).[8,9] Symmetry elements characteristic of the structure are consistent with the space group *Pnam* (the nonstandard setting is used to distinguish this phase from that isostructural with $LnFeO_3$ orthoferrites (S.G. *Pnma*)). In the unit cell (containing 16 formula units), *A*-site ions occupy two 4*c* and one 8*d* positions, iron—two 8*d* positions, oxygen—two 4*c* and five 8*d* positions.[17] Depending on investigation purposes, this complex structural model can be substituted by the simplified one neglecting the weak modulated in-phase/antiphase octahedral tilting and combining the antipolar displacements of the *A*-site cations with the simple $a^-a^-c^0$ tilting scheme.[8,9] Taking into account the similarity of the x-ray diffraction spectra obtained for the $Bi_{1-x}Nd_xFeO_3$ ($0.15 \le x \le 0.2$) solid solutions[8] and $Bi_{0.825}Nd_{0.175}Fe_{1-y}Mn_yO_3$ ($0.1 \le y \le 0.2$) samples (present work), the simplified model previously successfully applied to the $Bi_{0.825}Nd_{0.175}FeO_3$ ceramics[9] was used for the crystal structure refinement of the Mn-doped compounds. A good agreement between the observed and calculated XRD patterns obtained for the $y = 0.1$ samples is shown in Fig. 1. The refined structural data are summarized in Table I. Gradual decreasing of the intensity of the diffraction peaks originating from the antipolar displacements of the *A*-site cations takes place with increasing Mn concentration (right inset in Fig. 1). Character of the related structural changes (Mn doping-induced suppression of the displacements along the $[110/1\bar{1}0]_C$ directions of the parent cubic perovskite cell coincident with *a* axis of the orthorhombic unit cell) can be easily followed by comparing fractional coordinates of the Bi^{3+}/Nd^{3+} ions for the compounds with different *B*-sublattice composition (Table I). For y = 0.3 samples, additional diffraction peaks incompatible with the parent antiferroelectric structure were found. Rietveld refinement of the

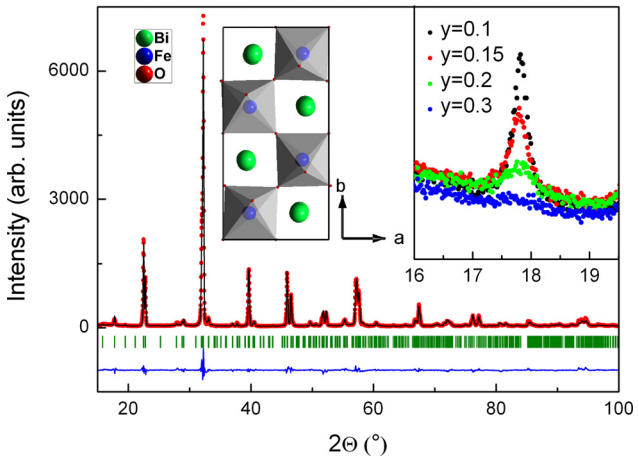

FIG. 1. Observed, calculated, and difference XRD patterns for $Bi_{0.825}Nd_{0.175}Fe_{0.9}Mn_{0.1}O_3$ compound at room temperature. Left inset shows schematic view of crystal structure of the y = 0.1 compound along [001] direction. Right inset demonstrates compositional variation of intensity of the diffraction peak (110) for $Bi_{0.825}Nd_{0.175}Fe_{1-y}Mn_yO_3$ ($0.1 \le y \le 0.3$) samples.

TABLE I. Structural parameters of the $Bi_{0.825}Nd_{0.175}Fe_{1-y}Mn_yO_3$ compounds at room temperature.

Composition space group	Cell (Å)	Atom	Site	x	y	z	R-factors (%)
$y = 0.1$	$a = 5.57885(4)$	Bi/Nd1	4g	0.7170(9)	0.1240(3)	0	$R_p = 7.64$
Pbam	$b = 11.20179(7)$	Bi/Nd2	4h	0.7222(9)	0.1321(2)	0.5	$R_{wp} = 10.6$
	$c = 7.80348(4)$	Fe/Mn	8i	0.2472(8)	0.1241(9)	0.250(3)	$R_B = 6.72$
		O1	4g	0.278(7)	0.183(3)	0	
		O2	4h	0.290(6)	0.114(3)	0.5	
		O3	8i	0.017(3)	0.2534(18)	0.300(3)	
		O4	4f	0	0.5	0.221(6)	
		O5	4e	0	0	0.244(9)	
$y = 0.2$	$a = 5.57308(3)$	Bi/Nd1	4g	0.7277(10)	0.1241(3)	0	$R_p = 8.17$
Pbam	$b = 11.17989(6)$	Bi/Nd2	4h	0.7355(10)	0.1340(3)	0.5	$R_{wp} = 10.8$
	$c = 7.80009(3)$	Fe/Mn	8i	0.2493(14)	0.1232(9)	0.250(3)	$R_B = 7.42$
		O1	4g	0.266(10)	0.178(3)	0	
		O2	4h	0.310(9)	0.121(4)	0.5	
		O3	8i	0.006(6)	0.249(3)	0.312(3)	
		O4	4f	0	0.5	0.240(15)	
		O5	4e	0	0	0.250(16)	

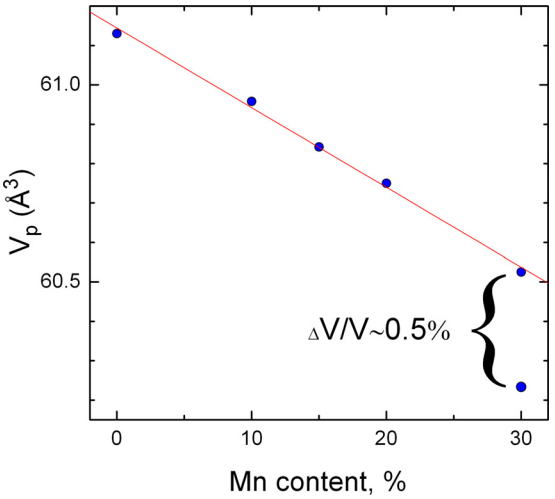

FIG. 2. Compositional dependence of the primitive cell volume for $Bi_{0.825}Nd_{0.175}Fe_{1-y}Mn_yO_3$ ($0 \le y \le 0.3$) series. Data for the $y = 0$ compound were taken from Ref. 9. Straight line is a linear fit reflecting a Vegard's law behavior.

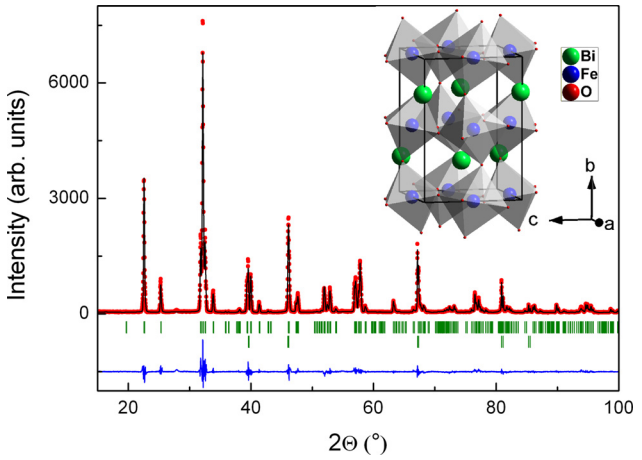

FIG. 3. Observed, calculated, and difference XRD patterns for $Bi_{0.825}Nd_{0.175}Fe_{0.85}Mn_{0.15}O_3$ compound at T = 300 °C. The bars mark the reflections positions for the main perovskite phase (top) and platinum holder (bottom). Inset illustrates the crystal structure of the perovskite compound.

compound confirmed that, apart from the antipolar phase, the $y = 0.3$ samples contain the nonpolar orthorhombic phase ($a^-b^+a^-$ tilting; space group *Pnma*) typical of Nd(Fe,Mn)O_3 perovskites (so-called $GdFeO_3$-type structure[18]). The structural transformation is accompanied by a step-like contraction of the primitive cell volume (by ~0.5%) characteristic of first-order transition (Fig. 2). Beyond the transition, primitive cell volume gradually decreases with increasing Mn concentration in accordance with changing the average ionic radius of the *B*-sublattice ions ($r_{\langle Mn^{3+}/Mn^{4+}\rangle} < r_{Fe^{3+}}$[19]). The same Mn substitution-driven structural phase transition was previously found in the $Bi_{0.86}Sm_{0.14}Fe_{1-y}Mn_yO_3$ series.[13] Comparison of the structural phase evolution in the antiferroelectric $Bi_{1-x}Ln_xFeO_3$ (Ln = La, Pr, Nd, Sm) compounds upon the Mn doping (Refs. 11–13 and present work) suggests that decreasing ionic radius of the substituting lanthanide hampers stabilization of the incommensurately modulated antipolar phase in the $Bi_{1-x}Ln_x$(Fe,Mn)O_3 series (this phase is typical for *Ln* = La and Pr) and shifts composition boundaries of the Mn doping induced *Pnam* → *Pnma* phase transition towards smaller *x*.

The reference compound, $Bi_{0.825}Nd_{0.175}FeO_3$, is known to undergo the temperature driven *Pnam* → *Pnma* phase transition at ~240 °C.[9] The same structural transformation is found to be realized in the Mn-doped series (Fig. 3, Table II). Differential scanning calorimetry carried out for the Mn-substituted samples (full scanning was performed in a range from 25 °C to 350 °C) shows that temperature of the structural transformation decreases with a close to constant rate of 5 °C per 1% Mn with increasing manganese content (Fig. 4). Pronounced hysteresis between the heating and cooling runs (up to 30 °C) indicates the first-order phase transition. The enthalpy associated with the transition (1 to 1.2 kJ/mol for the single-phase compounds with $y = 0.1$, 0.15, 0.2) is close to the values reported for isostructural $Bi_{1-x}Nd_xFe_{0.97}Ti_{0.03}O_3$ samples with the similar *A*-sublattice composition.[20] The much lower enthalpy value registered for the $y = 0.3$ compound (~0.3 kJ/mol) is consistent with the fact that the transformation must concern only one of the phases composing this structurally inhomogeneous sample. The heat anomalies characteristic of magnetic phase transition in the $BiFeO_3$-based compounds is known to be at least an order of magnitude smaller than those typical of the (anti)ferroelectric-paraelectric transition,[20] so we did not manage to detect them during the DSC measurements.

Structural phase diagram of the $Bi_{0.875}Nd_{0.175}Fe_{1-y}Mn_yO_3$ ($y \le 0.3$) system constructed using the XRD and DSC data is shown in Fig. 5. The concentration dependence of the *Pnam* → *Pnma* transition temperature in the $Bi_{0.875}Nd_{0.175}Fe_{1-y}Mn_yO_3$ series is very similar to that characteristic of the *R3c* → *Pnma* phase transition in the $BiFe_{1-y}Mn_yO_3$ system,[10] thus implying that changing the average ionic radius of the *B*-site elements or/and the substitution-induced disorder in the *B*-sublattice similarly affect the local dipole ordering (primarily associated with the stereochemical activity of the Bi^{3+} lone electron pair) in the polar and antipolar phases. It is worth noting that linear composition dependence of the (anti)ferroelectric transition temperature correlating with the average tolerance factor and average *A*-site polarizability was also observed in the $Bi_{1-x}Ln_xFeO_3$

TABLE II. Structural parameters of the $Bi_{0.825}Nd_{0.175}Fe_{0.85}Mn_{0.15}O_3$ compound at T = 300 °C.

Space group	Cell (Å)	Atom	Site	x	y	z	R-factors (%)
Pnma	$a = 5.61698(3)$	Bi/Nd	4c	0.04374(19)	0.25	0.9944(4)	$R_p = 8.03$
	$b = 7.86401(4)$	Fe/Mn	4b	0	0	0.5	$R_{wp} = 10.5$
	$c = 5.49615(2)$	O1	4c	0.480(3)	0.25	0.091(3)	$R_B = 5.29$
		O2	8d	0.187(2)	0.534(2)	0.192(2)	

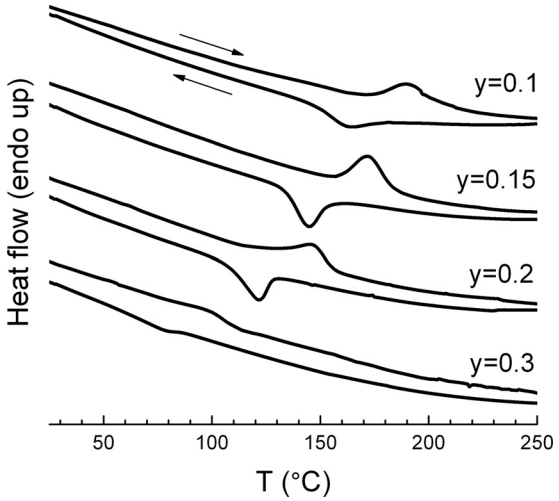

FIG. 4. Differential scanning calorimetry curves obtained for $Bi_{0.825}Nd_{0.175}Fe_{1-y}Mn_yO_3$ ($0.1 \le y \le 0.3$) samples.

series.[21] Our XRD and DSC data indicate that despite the opposite influence of the *A*-site Ln^{3+} and *B*-site Mn^{3+}/Mn^{4+} doping of $BiFeO_3$ on the Goldschmidt tolerance factor $t = \frac{r_A + r_O}{\sqrt{2}(r_B + r_O)}$, determining the degree of distortion in perovskites (r_A, r_B, and r_O are the ionic radii of *A*, *B*, and O ions; $r_{Ln^{3+}} < r_{Bi^{3+}}$, $r_{\langle Mn^{3+}/Mn^{4+}\rangle} < r_{Fe^{3+}}$), the composition and temperature controlled evolution of the antiferroelectric phase in the $Bi_{1-x}Nd_xFeO_3$ and $Bi_{0.875}Nd_{0.175}Fe_{1-y}Mn_yO_3$ systems tend to follow the same scenario (suppression of the antipolar displacements, decrease of the antipolar-to-nonpolar transition temperature and stabilization of the *Pnma* structure), thus suggesting a complex interplay between the electric dipole ordering associated with the stereochemical activity of $6s^2$ lone pairs of the Bi^{3+} ions and rotations/distorsions of the $\langle Fe,Mn\rangle O_6$ octahedra.

Magnetic properties of the $Bi_{0.825}Nd_{0.175}Fe_{1-y}Mn_yO_3$ compounds are mainly determined by exchange interactions between the *B*-site ions that are controlled by the overlap between the Fe/Mn *d*-orbitals and the O *p*-orbitals. The resulting superexchange interactions depend on the orbital configuration following the Goodenough–Kanamori rules.[22,23] These rules predict that the dominant superexchange interaction characteristic of the samples under study, Fe^{3+}: $t_{2g}^3e_g^2$–O–Fe^{3+}: $t_{2g}^3e_g^2$, must be antiferromagnetic. Accordingly, for the $y = 0$ compound, the ordered spins should create the isotropic *G*-type antiferromagnetic structure, in which each Fe^{3+} ion must be surrounded by six nearest neighbors with antiparallel magnetic moments. However, the Dzyaloshinsky–Moriya interaction[24,25] gives rise to a canting of the antiferromagnetic alignment of spins in the orthorhombic phases of the $Bi_{1-x}Ln_xFeO_3$ systems[26] to yield the small spontaneous magnetization of ~0.25–0.3 emu/g (at room temperature) for the *B*-site undoped $Bi_{0.825}Nd_{0.175}FeO_3$ perovskite.[9] Introducing the Mn ions into the host lattice should lead to the appearance of the competitive Mn^{3+}: $t_{2g}^3e_g^1$–O–Mn^{3+}: $t_{2g}^3e_g^1$ and Mn^{3+}: $t_{2g}^3e_g^1$–O–Mn^{4+}: $t_{2g}^3e_g^0$ ferromagnetic interactions that must strongly affect the magnetic behavior of the $Bi_{0.825}Nd_{0.175}Fe_{1-y}Mn_yO_3$ compounds. Fig. 6 illustrates the effect of the Mn doping. At room temperature, a close to linear decrease of the remanent/spontaneous magnetization (from ~0.22 emu/g for $y = 0.1$ to ~0.08 emu/g for $y = 0.3$) takes place with increasing Mn concentration (Fig. 6(a)). The behavior is consistent with a linear decrease of the Neel point observed in the $BiFe_{1-y}Mn_yO_3$ series that, in turn, correlates with changing the average number of e_g electrons on the *B* site.[10] The opposite situation is expectedly realized at low temperatures, where the spontaneous magnetization increases with increasing manganese content (Fig. 6(b)). The spontaneous magnetization values (from ~1 emu/g for $y = 0.1$ to ~3 emu/g for $y = 0.3$), as

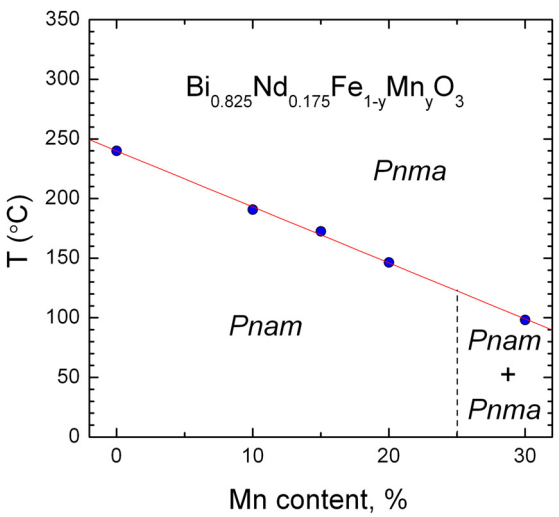

FIG. 5. Structural phase diagram of the $Bi_{0.875}Nd_{0.175}Fe_{1-y}Mn_yO_3$ ($0 \le y \le 0.3$) system. Transition temperature for the $y = 0$ compound was taken from Ref. 9.

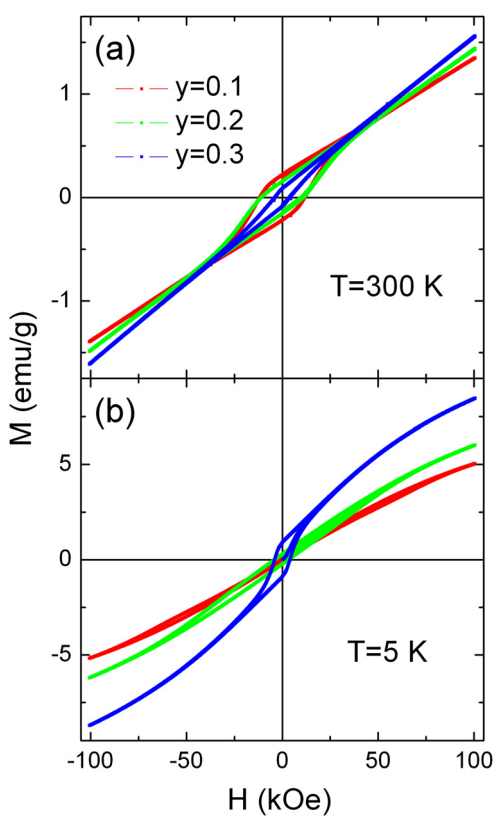

FIG. 6. Field dependences of the magnetization obtained for $Bi_{0.825}Nd_{0.175}Fe_{1-y}Mn_yO_3$ ($0.1 \le y \le 0.3$) compounds at T = 300 K (a) and T = 5 K (b).

extracted from the linear extrapolation of the high field magnetization to $H = 0$, are comparable with that characteristic of the $LaFe_{1-y}Mn_yO_3$ compounds with the close *B*-sublattice composition.[27]

IV. CONCLUSIONS

Effect of the Mn doping on the crystal structure and magnetic properties of the antiferroelectric phase (S.G. *Pnam*) of the $Bi_{1-x}Nd_xFeO_3$ perovskites was studied with x-ray diffraction, differential scanning calorimetry, and vibrational magnetometry techniques. The Mn substitution was found to gradually suppress the antipolar displacements of the Bi^{3+} ions characteristic of the low-doped $Bi_{0.825}Nd_{0.175}Fe_{1-y}Mn_yO_3$ compounds to induce the first-order $Pnam \rightarrow Pnma$ phase transition at $y \sim 0.3$. The same structural transformation is realized for the antiferroelectric phase at high temperature. The temperature of the $Pnam \rightarrow Pnma$ transition decreases with a close to constant rate of 5 °C per 1% Mn with increase of manganese content. Being consistent with lowering the Neel point in the $BiFe_{1-y}Mn_yO_3$ perovskites with increasing Mn concentration,[10] the *B*-site substitution gives rise to decrease of the room-temperature spontaneous magnetization in the $Bi_{0.825}Nd_{0.175}Fe_{1-y}Mn_yO_3$ series. Reflecting appearance of the competitive superexchange interactions induced by the Mn doping, the compositional dependence of the spontaneous magnetization oppositely changes at low temperature.

ACKNOWLEDGMENTS

This work was supported by funds from FEDER (Programa Operacional Factores de Competitividade COMPETE) and from FCT-Fundação para a Ciência e a Tecnologia under the project PEst-C/FIS/UI0036/2011, PEst-C/CTM/LA0011/2011, PTDC/FIS/105416/2008, program "Ciência 2008," and grants SFRH/BPD/42506/2007, SFRH/BPD/39262/2007. The authors would also like to acknowledge the financial support of the BRFFI (Grant T10R-119).

[1]W. Eerenstein, N. D. Mathur, and J. F. Scott, Nature **442**, 759 (2006).
[2]G. Catalan and J. F. Scott, Adv. Mater. **21**, 2463 (2009).
[3]I. Sosnowska, T. Peterlin-Neumaier, and E. Steichele, J. Phys. C **15**, 4835 (1982).
[4]Yu. F. Popov, A. K. Zvezdin, G. P. Vorob'ev, A. M. Kadomtseva, V. A. Murashev, and D. N. Rakov, JETP Lett. **57**, 69 (1993).
[5]Z. V. Gabbasova, M. D. Kuz'min, A. K. Zvezdin, I. S. Dubenko, V. A. Murashov, D. N. Rakov, and I. B. Krynetsky, Phys. Lett. A **158**, 491 (1991).
[6]A. W. Hewat, Ferroelectrics **7**, 83 (1974).
[7]A. M. Glazer, K. Roleder, and J. Dec, Acta Crystallogr., Sect. B: Struct. Sci. **49**, 846 (1993).
[8]S. Karimi, I. M. Reaney, I. Levin, and I. Sterianou, Appl. Phys. Lett. **94**, 112903 (2009).
[9]I. Levin, M. G. Tucker, H. Wu, V. Provenzano, C. L. Dennis, S. Karimi, T. Comyn, T. Stevenson, R. I. Smith, and I. M. Reaney, Chem. Mater. **23**, 2166 (2011).
[10]S. M. Selbach, T. Tybell, M.-A. Einarsrud, and T. Grande, Chem. Mater. **21**, 5176 (2009).
[11]V. A. Khomchenko, I. O. Troyanchuk, D. V. Karpinsky, S. Das, V. S. Amaral, M. Tovar, V. Sikolenko, and J. A. Paixão, "Structural transitions and unusual magnetic behavior in Mn-doped $Bi_{1-x}La_xFeO_3$ perovskites," J. Appl. Phys. (submitted).
[12]V. A. Khomchenko, I. O. Troyanchuk, M. I. Kovetskaya, M. Kopcewicz, and J. A. Paixão, J. Phys. D: Appl. Phys. **45**, 045302 (2012).
[13]V. A. Khomchenko, I. O. Troyanchuk, M. I. Kovetskaya, and J. A. Paixão, J. Appl. Phys. **111**, 014110 (2012).
[14]S. Saxin and C. S. Knee, Dalton Trans. **40**, 3462 (2011).
[15]J. Rodríguez-Carvajal, Physica B **192**, 55 (1993).
[16]A. M. Glazer, Acta Crystallogr., Sect. A: Cryst. Phys., Diffr., Theor. Gen. Crystallogr. **31**, 756 (1975).
[17]M. Kubota, K. Oka, Y. Nakamura, H. Yabuta, K. Miura, Y. Shimakawa, and M. Azuma, Jpn. J. Appl. Phys.,Part 1 **50**, 09NE08 (2011).
[18]S. Geller, J. Chem. Phys. **24**, 1236 (1956).
[19]R. D. Shannon, Acta Crystallogr., Sect. A: Cryst. Phys., Diffr., Theor. Gen. Crystallogr. **32**, 751 (1976).
[20]K. Kalantari, I. Sterianou, D. C. Sinclair, P. A. Bingham, J. Pokorny, and I. M. Reaney, J. Appl. Phys. **111**, 064107 (2012).
[21]S. Karimi, I. M. Reaney, Y. Han, J. Pokorny, and I. Sterianou, J. Mater. Sci. **44**, 5102 (2009).
[22]J. B. Goodenough, Phys. Rev. **100**, 564 (1955).
[23]J. Kanamori, J. Phys. Chem. Solids **10**, 87 (1959).
[24]I. Dzyaloshinsky, J. Phys. Chem. Solids **4**, 241 (1958).
[25]T. Moriya, Phys. Rev. **120**, 91 (1960).
[26]V. A. Khomchenko, L. C. J. Pereira, and J. A. Paixão, J. Phys. D: Appl. Phys. **44**, 185406 (2011).
[27]O. F. de Lima, J. A. H. Coaquira, R. L. de Almeida, L. B. de Carvalho, and S. K. Malik, J. Appl. Phys. **105**, 013907 (2009).